# Hydridogallium Bis(tetrahydroborate) in the Gas Phase: Vibrational Properties and Structure Determined by Electron Diffraction and *ab Initio* and Density Functional Theory Computations

**Anthony J. Downs,* Tim M. Greene, Lisa A. Harman, and Philip F. Souter**

Inorganic Chemistry Laboratory, University of Oxford, South Parks Road, Oxford, OX1 3QR, U.K.

**Paul T. Brain, Colin R. Pulham, David W. H. Rankin, and Heather E. Robertson**

Department of Chemistry, University of Edinburgh, West Mains Road, Edinburgh, EH9 3JJ, U.K.

**Matthias Hofmann and Paul von Ragué Schleyer**

Computer-Chemie-Centrum des Instituts für Organische Chemie, Universität Erlangen-Nürnberg, Nägelsbachstrasse 25, D-91052 Erlangen, Germany

*Received August 30, 1994*[⊗]

The "mixed" gallium−boron hydride $HGa(BH_4)_2$ in its isotopically natural and perdeuteriated versions has been characterized both experimentally, by gas-phase electron diffraction and vibrational spectroscopy, and through *ab initio* [MP2(fc)/SV(d) level] and density functional theory [Becke3LYP/TZ(d, p) level] calculations. The vapor consists of monomeric $HGa(BH_4)_2$ molecules with a single terminal Ga−H bond and two bidentate $BH_4$ groups. The electron-diffraction pattern of the vapor has been remeasured using an all-glass inlet system. The theoretically favored model with $C_{2v}$ symmetry provides the most satisfactory fit to the data. The following parameters ($r_a$ structure, distances in pm, angles in degrees; $H_t$ terminal H atom, $H_b$ bridging H atom) have been determined: $r$(Ga−$H_t$) 150(4), $r$(Ga−$H_b$) 178.8(7), $r$(Ga−B) 218.5(2), $r$(B−$H_t$) 118.4(4), $r$(B−$H_b$) 126.7(4), and B−Ga−B 119.2(15). The physical and spectroscopic properties of the compound imply that loose aggregation occurs in the condensed phases.

## Introduction

Gallium tetrahydroborates remained relatively poorly characterized[1,2] until 1976−1978 when the compounds $Me_2GaBH_4$[3] and $HGa(BH_4)_2$[4] were described in some detail. The latter attracted attention as a rare example of an uncoordinated gallium hydride, but the highly reactive nature of this hydridogallium derivative complicated the collection of good electron-diffraction patterns. Nevertheless, the gas-phase structure was eventually determined.[5] The results provided strong evidence for a

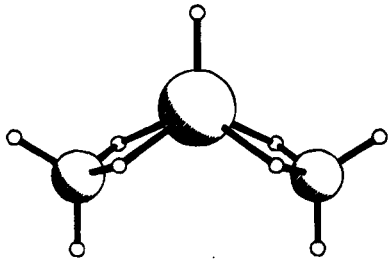

**1**

monomeric $HGa(BH_4)_2$ molecule **1** with 5-fold coordination of the gallium atom, a single terminal Ga−H bond, and two doubly bridged $BH_4$ groups, but left open the *exact* form of the Ga($\mu$-$H)_2$B groups.[5] The best refinement implied a $C_2$ model having asymmetric Ga($\mu$-$H)_2$B bridges with one long [189.1(25) pm] and one short [176.2(15) pm] Ga−$H_b$ bond ("b" denotes bridging atom). Some support for such a model came from a general theoretical study of group IIIA hydrides[6] which found that $M_3H_9$ trimers (M = B, Al, Ga) have access to pentacoordinated structures of the HM[($\mu$-$H)_2MH_2]_2$ type, similar to **1**, as either an energy minimum (M = Al) or a transition state (M = Ga) on the potential hypersurface. However, isomers of type **2** incorporating a planar six-membered ring in which the

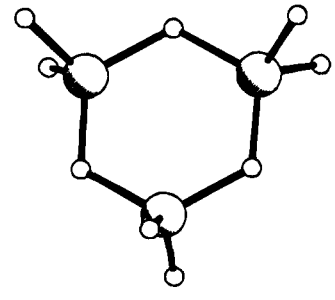

**2**

M atoms are linked through *single* hydrogen bridges were

* Author to whom correspondence should be addressed.

[⊗] Abstract published in *Advance ACS Abstracts,* February 15, 1995.

(1) Nöth, H. *Angew. Chem.* **1961**, *73*, 371. Wiberg, E.; Amberger, E. *Hydrides of the Elements of Main Groups I-IV*; Elsevier: Amsterdam, 1971.

(2) James, B. D.; Wallbridge, M. G. H. *Prog. Inorg. Chem.* **1970**, *11*, 99. Marks, T. J.; Kolb, J. R. *Chem. Rev.* **1977**, *77*, 263.

(3) Downs, A. J.; Thomas, P. D. P. *J. Chem. Soc., Dalton Trans.* **1978**, 809.

(4) Downs, A. J.; Thomas, P. D. P. *J. Chem. Soc., Chem. Commun.*, **1976**, 825.

(5) Barlow, M. T.; Dain, C. J.; Downs, A. J.; Laurenson, G. S.; Rankin, D. W. H. *J. Chem. Soc., Dalton Trans.* **1982**, 597.

0020-1669/95/1334-1799$09.00/0 

more stable. The pentacoordinated structures are very similar to the $C_2$ model for the mixed hydride $GaB_2H_9$ with asymmetric coordination of the $MH_4$ moieties to the central M atom (the $Al-H_b$ distances being 182 and 170 pm and the $Ga-H_b$ distances even more disparate at *ca.* 210 and 165 pm).[6]

Interest in the ligation of $BH_4^-$ has been heightened recently, not only by the discovery in $Ti(BH_4)_3(PMe_3)_2$ of new variations on the familiar themes of mono-, bi-, and tridentate coordination,[7] but also by its potential relevance to the activation of the isoelectronic $CH_4$ molecule.[8] Hydridogallium bis(tetrahydroborate) is also noteworthy in being a volatile compound which decomposes to gallium metal at ambient temperatures. In this respect, it resembles the parent gallium hydride, $[GaH_3]_n$,[9] and gallaborane, $[H_2GaBH_4]_n$.[10,11] Not only do such compounds offer a means of vapor transport of pure gallium at low temperatures (< 273 K), they may well model intermediates formed in the complex thermolysis reactions attending chemical vapor deposition and terminating in solid gallium-bearing films.[12]

In this paper we describe the vibrational spectra of hydridogallium bis(tetrahydroborate) in its normal and perdeuteriated forms. The spectra of the vapor are consistent with the presence of an $HGa(BH_4)_2$ molecule, **1**, with $C_{2v}$ symmetry and symmetrical bidentate coordination of the $BH_4$ ligands. *Ab initio* and density functional theory calculations at the MP2(fc)/SV(d) and Becke3LYP/TZ(d, p) level, respectively, yield a harmonic force field, vibrational frequencies, and infrared intensities in remarkably close agreement with the experimental results. The electron-diffraction pattern of the vapor has been remeasured using an all-glass inlet system, and these results have been analyzed, in conjunction with the vibrational properties and the results of the theoretical computations, in a reassessment of the structure adopted by the gaseous molecule.

## Experimental Section

**Synthesis of Hydridogallium Bis(tetrahydroborate).** Hydridogallium bis(tetrahydroborate) was prepared by the reaction between gallium(III) chloride (prepared by the direct reaction of the elements and purified by repeated vacuum sublimation) and freshly recrystallized lithium tetrahydroborate. In one such experiment, a specially constructed double-limbed reaction vessel was used to enable 2.0 g (11.4 mmol $GaCl_3$) of the powdered chloride to be tipped onto 1.0 g (46 mmol) of $LiBH_4$ which, together with a glass-coated magnetic "flea", was held in the main reaction chamber at 77 K. The reaction mixture was allowed to warm *in vacuo* under solvent- and grease-free conditions. When the temperature reached 238 K, a reaction set in. The volatile products [$H_2$, $B_2H_6$, and $HGa(BH_4)_2$] were removed under continuous pumping and the condensable components were trapped at 77 K. The mixture was allowed to warm slowly to 263 K over 4–5 h (the magnetic "flea" was used to promote mixing of the reagents) until the reaction appeared to be complete. Fractional condensation of the condensable volatile products through traps held at 228, 190, and 77 K gave a fraction collected at 190 K which was judged to be pure hydridogallium bis(tetrahydroborate) on the basis of its vapor pressure and IR and NMR spectra. This fraction amounted to 740 mg (7.4 mmol) of the bis(tetrahydroborate), representing a 65% yield based on the quantity of gallium chloride consumed, in accord with eq 1.The

$$^1/_2Ga_2Cl_6 + 3LiBH_4 \rightarrow HGa(BH_4)_2 + 3LiCl + {}^1/_2B_2H_6 \quad (1)$$

$HGa(BH_4)_2$ product was stored at 77 K in a sealed, evacuated all-glass ampule equipped with a break-seal. The deuteriated derivative, [$^2H_9$]-hydridogallium bis(tetrahydroborate), was synthesized similarly from gallium(III) chloride and $LiBD_4$.

As in other experiments leading to the synthesis of uncoordinated gallane and its derivatives,[9,11,13] success depended crucially on the preconditioning of all the glassware used by heating under continuous pumping and on the rigor with which moisture and other impurities were excluded from the apparatus. Although the earlier experiments were carried out in apparatus equipped with greaseless valves, and the hydridogallium bis(tetrahydroborate) was even manipulated briefly in apparatus including components sealed and lubricated with Apiezon L grease, the best results were achieved with an all-glass apparatus analogous to that employed for the synthesis of gallane.[9,11] However, as hydridogallium bis(tetrahydroborate) is less sensitive to thermal decomposition than gallane, it was not necessary to cool all the glassware to which the vapor had access.[8,10]

**Chemical Analysis of Hydridogallium Bis(tetrahydroborate).** A sample of the gallane, allowed to decompose at room temperature for 24 h, deposited gallium metal on the walls of the ampule. The temperature was then raised to 333 K for 2 h to ensure completeness of reaction. The volatile products were withdrawn and the diborane was trapped at 77 K, prior to tensimetric assay and IR characterization,[14] while the dihydrogen was collected and assayed by means of a Toepler pump. Analysis showed that the grey involatile residue was elemental gallium. In a typical experiment 89.4 mg (0.890 mmol) of the gallane yielded 0.880 mmol of $B_2H_6$, 1.35 mmol of $H_2$, and 65.8 mg (0.944 mmol) of Ga metal, corresponding to the proportions gallane:$B_2H_6$:$H_2$:Ga = 1:0.99:1.52:1.06 and consistent, within the limits of experimental error, with the stoicheiometry of eq 2.

$$HGa(BH_4)_2 \rightarrow Ga + {}^3/_2H_2 + B_2H_6 \quad (2)$$

**Spectroscopic Measurements.** IR spectra were recorded using four spectrometers, *viz.* Perkin-Elmer 225 and 580A dispersive instruments (4000–200 $cm^{-1}$) and Mattson Polaris and Galaxy FT-IR instruments (4000–400 $cm^{-1}$). Solid argon or nitrogen matrices, typically at dilutions estimated to be *ca.* 1:200, were prepared by continuous deposition of the gallane vapor with an excess of the matrix gas on a CsI window cooled to *ca.* 12 K by means of a Displex closed-cycle refrigerator (Air Products Model CS 202); fuller details of the relevant equipment and procedures are given elsewhere.[15] Raman spectra were excited at $\lambda$ = 514.5 nm with the output of a Spectra-Physics Model 165 $Ar^+$ laser and measured with a Spex Ramalog 5 spectrophotometer; the resolution was normally *ca.* 5 $cm^{-1}$. Solid films of volatile materials were presented for spectroscopic analysis by causing the vapor to condense on a CsI window (for IR measurements) or a copper block (for Raman measurements) contained in an evacuated shroud and maintained at 77 or 20 K, respectively.

**Electron-Diffraction Measurements.** The Edinburgh gas-diffraction apparatus was used for the electron-diffraction measurements, the patterns being recorded on Kodak Electron Image plates.[16] Because of the reactivity and thermal frailty of hydridogallium bis(tetrahydroborate), we avoided both valves and joints by employing the special all-glass inlet assembly described previously.[9b] The measurements were

(6) Duke, B. J.; Liang, C.; Schaefer, H. F., III. *J. Am. Chem. Soc.* **1991**, *113*, 2884.
(7) Jensen, J. A.; Girolami, G. S. *J. Chem. Soc., Chem. Commun.* **1986**, 1160. Jensen, J. A.; Wilson, S. R.; Girolami, G. S. *J. Am. Chem. Soc.* **1988**, *110*, 4977.
(8) Saillard, J.-Y.; Hoffmann, R. *J. Am. Chem. Soc.* **1984**, *106*, 2006.
(9) (a) Downs, A. J.; Goode, M. J.; Pulham, C. R. *J. Am. Chem. Soc.* **1989**, *111*, 1936. (b) Pulham, C. R.; Downs, A. J.; Goode, M. J.; Rankin, D. W. H.; Robertson, H. E. J. *Am. Chem. Soc.* **1991**, *113*, 5149.
(10) Pulham, C. R.; Brain, P. T.; Downs, A. J.; Rankin, D. W. H.; Robertson, H. E. *J. Chem. Soc., Chem. Commun.* **1990**, 177.
(11) Pulham, C. R. D.Phil. Thesis, University of Oxford, 1991.
(12) Moss, R. H. *Chem. Br.* **1983**, *19*, 733. Cole-Hamilton, D. J. *Chem. Br.* **1990**, *26*, 852. Wee, A. T. S.; Murrell, A. J.; Singh, N. K.; O'Hare, D.; Foord, J. S. *J. Chem. Soc., Chem. Commun.* **1990**, 11. Tsang, W. T. *J. Cryst. Growth* **1992**, *120*, 1. Foord, J. S.; Wee, A. T. S.; Singh, N. K.; Whitaker, T. J.; O'Hare, D. *Mater. Res. Soc. Symp. Proc.* **1992**, *282*, 27. Gee, P. E.; Hicks, R. F. *J. Vac. Sci. Technol., A* **1992**, *10*, 892. Qi, H.; Gee, P. E.; Hicks, R. F. *Phys. Rev. Lett.* **1994**, *72*, 2500.
(13) Downs, A. J.; Pulham, C. R. *Adv. Inorg. Chem.* **1994**, *41*, 171.
(14) Duncan, J. L.; McKean, D. C.; Torto, I.; Nivellini, G. D. *J. Mol. Spectrosc.* **1981**, *85*, 16.
(15) For example, see: Hawkins, M.; Downs, A. J. *J. Phys. Chem.* **1984**, *88*, 1527, 3042.
(16) Huntley, C. M.; Laurenson, G. S.; Rankin, D. W. H. *J. Chem. Soc., Dalton Trans.* **1980**, 954.

**Table 1.** Nozzle-to-Plate Distances, Weighting Functions, Correlation Parameters, Scale Factors, and Electron Wavelengths[a]

| nozzle-to-plate distance/mm | weighting functions/nm$^{-1}$ $\Delta s$ | $s_{min}$ | $sw_1$ | $sw_2$ | $s_{max}$ | correln param | scale factor, $k$[a] | electron wavelength[b]/pm |
|---|---|---|---|---|---|---|---|---|
| 259.48 | 2 | 20 | 40 | 140 | 162 | 0.246 | 0.907(23) | 5.672 |
| 201.27 | 4 | 40 | 60 | 170 | 196 | −0.280 | 0.839(27) | 5.671 |

[a] Figures in parentheses are the estimated standard deviations. [b] Determined by reference to the scattering pattern of benzene vapor.

carried out at two camera distances, *viz.* ca. 201 and 260 mm, at an electron wavelength near 5.67 pm, and gave results spanning the range 20−196 nm$^{-1}$ in the scattering variable $s$. The ampule containing the sample was kept at 238 K, and the inlet system, preconditioned by preliminary exposure to a portion of the vapor, was cooled to temperatures in the range 260−266 K to minimize the risk of thermal decomposition. The rotating sector was kept in motion until all of the sample in the chamber had condensed in the cold trap to prevent an image of the stationary sector from being superimposed on the photographic plate. The plate was fogged, but had a homogeneous background. Each exposed plate was pumped on for 2 h, and was then removed, washed, and left in the air for 24 h before being developed. These procedures minimized the fogging due to the reaction of the gallane vapor with the photographic emulsion. The precise nozzle-to-plate distances and electron wavelengths were determined from scattering patterns for benzene vapor recorded immediately after the sample pattern. Details are given in Table 1, together with the weighting functions used to set up the off-diagonal weight matrix, the correlation parameters, and final scale factors.

Two plates recorded with a nozzle-to-plate distance of 201 mm and three recorded at 260 mm were selected for analysis. Details of the electron-scattering patterns were collected in digital form using a computer-controlled Joyce-Loebl MDM6 microdensitometer. The scanning program[17] and those for data reduction[17] and least-squares refinement[18] have been described previously. The complex scattering factors were those listed by Ross, Fink, and Hilderbrandt.[19]

**Theoretical Calculations.** *Ab initio* and density functional theory (DFT) optimizations in the chosen symmetry employed standard procedures using the Gaussian92[20,21] and Gaussian92/DFT programs,[20−22] respectively. *Ab initio* calculations were performed at the HF and MP2 levels of theory [the latter in the frozen core (fc) approximation]; the DFT computations employed the Becke3LYP method as implemented in Gaussian92/DFT.[22a] This is a slight variation of Becke's three-parameter hybrid functional[22b] and is based on the following functionals: (i) Slater exchange; (ii) Hartree-Fock exchange; (iii) Becke's 1988 exchange functional correction;[22c] (iv) the gradient-corrected correlation functional of Lee, Yang, and Parr;[22d] (v) the local correlation functional of Vosko, Wilk, and Nusair.[22e] The split-valence (SV) basis set of Alhrichs *et al.*[23] was used with the following additional polarization functions: d-type on the heavy atoms (B, 0.600; Ga, 0.207) for the *ab initio*, denoted SV(d), and d-type on the heavy atoms and p-type on the hydrogen atoms (B, 0.401; Ga, 0.207; H, 0.750), denoted TZ(d, p) for the DFT computations. Relative energies and cartesian force constants were calculated at the MP2/SV(d) and Becke3LYP/TZ(d, p) levels of theory. For the DFT computations, geometries were optimized using the Gaussian defaults while relative energies were derived from subsequent single-point energy calculations using the finegrid option in the numerical integration. Unless stated otherwise, values given in the text refer to DFT results. The calculations were performed on a Cray YMP-8 at the Höchstleistungs rechenzentrum in Jülich, Germany.

DFT computations consume less CPU time than traditional *ab initio* jobs at the MP2 level. Thus, a much larger basis set could be employed in the DFT calculations for $HGa(BH_4)_2$: TZ(d, p)−135 basis functions; SV(d)−78 basis functions. Consequently, there was little difference in the time between the Becke3LYP/TZ(d, p) and MP2/SV(d) level for one cycle of optimization. However, in the present implementation, optimizations with DFT methods require many more cycles to reach convergence of the geometry. DFT frequency computations were approximately 2.5 times the duration of those at the MP2 level.

## Results and Discussion

**(i) Vibrational Spectra. (a) Analysis of the Observed Spectra.** IR Spectra have been measured for the $HGa(BH_4)_2$ and $DGa(BD_4)_2$ vapors at low pressures (*ca.* 10 mmHg) and ambient temperatures, for the $HGa(BH_4)_2$ condensed from the gas phase into solid nitrogen or argon matrices at *ca.* 12 K and for the annealed solid condensates of $HGa(BH_4)_2$ and $DGa(BD_4)_2$ on a CsI window at 77 K. Raman spectra have also been measured for solid condensates on a copper block at 20 K. Measurements on liquid $HGa(BH_4)_2$ at 223 K revealed only two bands (at 1997 and 2047 cm$^{-1}$) and were thwarted partly by evaporation of the sample and partly by the low scattering cross-section of most of the vibrational transitions. Selected spectra are illustrated in Figure 1, and the details are given in Tables 2 and 3. Wavenumbers quoted in parentheses in the ensuing discussion refer to the perdeuteriated compound; the terms "in-plane" and "out-of-plane" relate to the $GaB_2$ skeleton.

The density and mass spectrum of hydridogallium bis(tetrahydroborate) vapor indicate that it consists predominantly of monomeric molecules $GaB_2H_9$, consistent with the electron-diffraction pattern as reported earlier.[5] The IR spectrum is most easily interpreted in terms of the $C_{2v}$ model (Figure 2) with 5-fold coordination of the gallium atom with two equivalent dihydrogen-bridged $BH_4$ groups; the terminal $BH_2$ moieties are coplanar with the heavy-atom $GaB_2$ skeleton. Not only are the spectral features characteristic of bidentate $BH_4$ groups evident,[2,3,24,25] but there are additional bands (near 2000, 730, and 630 cm$^{-1}$) which are most plausibly identified with stretching or bending motions of a terminal Ga−H unit. The 30 vibrational fundamentals are accommodated by the representation $10a_1 + 5a_2 + 9b_1 + 6b_2$; all are Raman-active and all but the $5a_2$ modes are IR active. The molecule is a near-prolate asymmetric top with the $GaB_2$ plane containing the axes of $I_A$ and $I_B$. The principal moments of inertia of the molecule have been estimated from the dimensions deduced in the earlier electron-diffraction studies:[5] $I_A = 41.96$, $I_B = 110.66$, and $I_C = 143.47$ amu Å$^2$ (1 amu = 1.6605 × 10$^{-27}$ kg). With the choice of coordinate axes shown in Figure 2, $a_1$ modes are expected to give rise in IR absorption to type-B, $b_1$ modes to type-A, and $b_2$ modes to type-C bands. Type A bands should be recognizable by P-, Q-, and R-branches of comparable intensity and a

(17) Cradock, S.; Koprowski, J.; Rankin, D. W. H. *J. Mol. Struct.* **1981**, *77*, 113.
(18) Boyd, A. S. F.; Laurenson, G. S.; Rankin, D. W. H. *J. Mol. Struct.* **1981**, *71*, 217.
(19) Ross, A. W.; Fink, M.; Hilderbrandt, R. In *International Tables for Crystallography*; Wilson, A. J. C., Ed.; Kluwer Academic Publishers: Dordrecht, The Netherlands, Boston, MA, and London, 1992; Vol. C, p 245.
(20) Frisch, M. J.; Trucks, G. W.; Schlegal, H. B.; Gill, P. M. W.; Johnson, B. J.; Wong, M. W.; Foresman, J. B.; Robb, M. A.; Head-Gordon, M.; Replogle, E. S.; Gomperts, R.; Andres, J. L.; Raghavachari, K.; Binkley, J. S.; Gonzalez, C.; Martin, R. L.; Fox, D. J.; DeFrees, D. J.; Baker, J.; Stewart, J. J. P.; Pople, J. A. Gaussian 92/DFT, Revision F.2. Gaussian Inc., Pittsburgh, PA, 1993.
(21) For an introduction to computational chemistry see, for example: (a) Foreman, J.; Frisch, Æ. *Exploring Chemistry with Electronic Structure Methods: A Guide to Using Gaussian*; Gaussian Inc.: Pittsburgh, PA, 1993. (b) Hehre, W. J.; Radom, L.; Schleyer, P. v. R.; Pople, J. A. *Ab Initio Molecular Orbital Theory*; Wiley: New York, 1986.
(22) (a) Stevens, P. J.; Devlin, F. J.; Chablowski, C. F.; Frisch, M. J. *J. Chem. Phys.*, submitted for publication. (b) Becke, A. D. *J. Chem. Phys.* **1993**, *98*, 5648. (c) Becke, A. D. *Phys. Rev. B* **1988**, *38*, 3098. (d) Lee, C.; Yang, W.; Parr, R. G. *Phys. Rev. B* **1988**, *37*, 785. (e) Vosko, S. H.; Wilk, L.; Nusair, M. *Can. J. Phys.* **1980**, *58*, 1200.
(23) Schäfer, A.; Horn, H.; Alhrichs, R. *J. Chem. Phys.* **1992**, *97*, 2571.
(24) Marks, T. J.; Kennelly, W. J.; Kolb, J. R.; Shimp, L. A. *Inorg. Chem.* **1972**, *11*, 2540.
(25) Coe, D. A.; Nibler, J. W. *Spectrochim. Acta, Part A* **1973**, *29*, 1789.

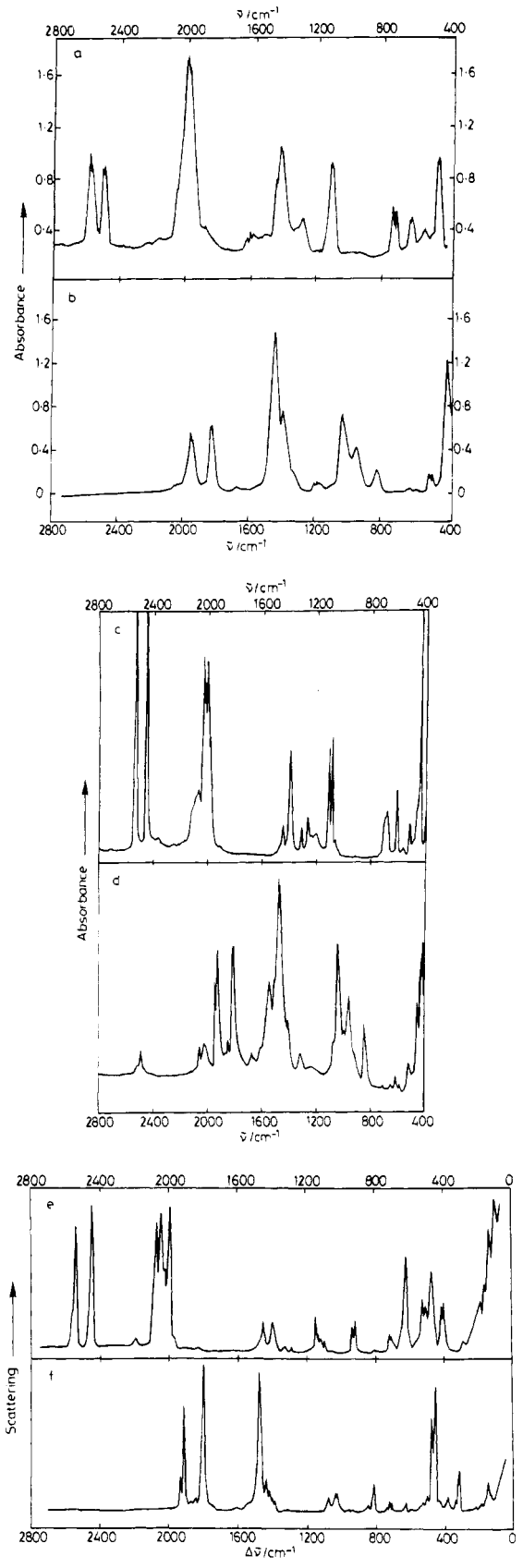


**Figure 1.** Vibrational spectra for $HGa(BH_4)_2$ and $DGa(BD_4)_2$: (a and b) IR spectra of $HGa(BH_4)_2$ and $DGa(BD_4)_2$ vapors, respectively: pressure *ca.* 10 mmHg and at room temperature (contained in a cell with CsI windows and having a path length of 10 cm). (c and d) IR spectra of partially annealed solid films of $HGa(BH_4)_2$ and $DGa(BD_4)_2$, respectively, at 77 K. (e and f) Raman spectra of partially annealed solid films of $HGa(BH_4)_2$ and $DGa(BD_4)_2$, respectively, at 20 K.

P−R separation, $\Delta\nu$(P−R), of *ca.* 18.5 $cm^{-1}$, and type-B and type-C bands by envelopes with a doublet structure [$\Delta\nu$(P-R) = *ca.* 15 $cm^{-1}$] and a prominent Q-branch [$\Delta\nu$(P−R) = *ca.* 28 $cm^{-1}$], respectively.[26]

On condensation at low temperatures, solid films of hydridogallium bis(tetrahydroborate) gave IR and Raman spectra quite similar to those observed for discrete $HGa(BH_4)_2$ [$DGa(BD_4)_2$] molecules. However, progressive annealing of the deposits led to changes in the spectra consistent with aggregation of these molecules. Table 3 lists the principal features of the monomer spectra. Further annealing resulted in changes of wavenumber and relative intensity and in the merging of bands due to the antisymmetric and symmetric stretching vibrations of the terminal B−H bonds. The changes in the spectra suggest the gradual formation of a weakly bound polymer. Here, as in the gaseous molecule (*q.v.*), bidentate coordination of the $BH_4$ groups appears to be maintained,[2,3,24,25] and it is likely that aggregation proceeds through the formation of Ga-H-Ga bridges analogous to those found in gallane, $[GaH_3]_n$,[9,11,13] and dimethylgallane, $[Me_2GaH]_n$.[27] In the final stages of annealing, the IR spectrum of the solid showed distinct similarities to the spectrum of the corresponding alane, $[HAl(BH_4)_2]_n$, which is an involatile, viscous liquid at normal temperatures.[28] Like the alane, but unlike the gaseous $HGa(BH_4)_2$ molecule, the solid gallane is then characterized by an intense absorption near 704 $cm^{-1}$ which—to judge by its marked response to deuteriation—probably represents a Ga−H−Ga or Ga−H−B vibration of the aggregate. In these conditions, the gallane may well adopt a structure akin to that of the alane in which Al−H−Al bridging is believed to complete 6-fold coordination of the metal center.[28]

Our interpretation leads to the vibrational assignments given in Tables 4 and 5. The analysis has been based on five main criteria: (*a*) the selection rules expected to govern the activity of modes in IR absorption; (*b*) the effect of deuteriation on the energy of a given spectroscopic transition; (*c*) the envelope of the IR absorption displayed by the vapor (*vide infra*); (*d*) analogies with the vibrational properties of related molecules, notably $Al(BH_4)_3$,[25] $Me_2GaBH_4$,[3] and $H_2GaBH_4$;[11] and (*e*) comparisons with the results of the *ab initio* and DFT calculations. We attach particular weight to the theoretical forecast and to comparisons with the relatively simple gaseous molecule $H_2GaBH_4$ which has been studied by *ab initio* calculations[29] and by rovibrational analysis, leading to unequivocal identification of most of the vibrational fundamentals.[11]

The spectrum of the bis(tetrahydroborate), $HGa(BH_4)_2$, is more complicated. First, there are now in-phase and out-of-phase versions of each fundamental associated with a $Ga(\mu\text{-}H)_2BH_2$ moiety, but, since vibrational coupling between the two coordinated $BH_4$ groups is likely to be weak, the two versions are almost equienergetic. Second, there are two isotopes, $^{10}B$ and $^{11}B$, in naturally occurring boron. Consequently, many bands overlap and so impair the potential usefulness of band envelopes as a guide to assignment. Contamination is another source of confusion with a compound as reactive and thermally fragile as $HGa(BH_4)_2$. Small concentrations of $H_2GaBH_4$, $B_2H_6$, chlorogallanes, and other impurities are difficult to exclude. The sample of $DGa(BD_4)_2$ was certainly contaminated with small

(26) Seth Paul, W. A.; Dijkstra, G. *Spectrochim. Acta, Part A* **1967**, *23*, 2861. Seth Paul, W. A. *J. Mol. Struct.* **1969**, *3*, 403.
(27) Baxter, P. L.; Downs, A. J.; Goode, M. J.; Rankin, D. W. H.; Robertson, H. E. *J. Chem. Soc., Chem. Commun.* **1986**, 805; *J. Chem. Soc., Dalton Trans.* **1990**, 2873.
(28) Downs, A. J.; Jones, L. A. *Polyhedron*, in press. Jones, L. A. D.Phil. Thesis, University of Oxford, 1993
(29) Van der Woerd, M. J.; Lammertsma, K.; Duke, B. J.; Schaefer III, H. F. *J. Chem. Phys.* **1991**, *95*, 1160.

**Table 2.** Principal Features in the IR Spectra of Gaseous and Matrix-Isolated Hydridogallium Bis(tetrahydroborate) and Gaseous [$^2H_9$]Hydridogallium Bis(tetrahydroborate)

| $HGa(BH_4)_2$ matrix-isolated at *ca.* 20 K | | | | vapor at *ca.* 290 K | | | | | | |
|---|---|---|---|---|---|---|---|---|---|---|
| $N_2$ matrix | | Ar matrix | | $HGa(BH_4)_2$ | | | $DGa(BD_4)_2$ | | | |
| $\tilde{\nu}$/cm$^{-1}$ | intens[a] | $\tilde{\nu}$/cm$^{-1}$ | intens[a] | $\tilde{\nu}$/cm$^{-1}$ | intens[a] | | $\tilde{\nu}$/cm$^{-1}$ | intens[a] | | assignment |
| | | | | | | | 1962 | sh | | |
| 2557 | m | 2580 | m | 2566 | s | B | 1940 | s | B | $\nu$(B−$H_t$) $\nu_1$ ($a_1$), $\nu_{16}$ ($b_1$) |
| 2534 | m | 2534 | m | 2550 | s | B | 1927 | s | B | |
| | | | | 2518 | w | | | | | *ca.* 1417 + 111 |
| 2481 | m | 2500 | mw | 2488 | s,R | A | 1822 | s,R | A | |
| 2464 | m | 2481 | mw | 2478 | s,Q | A | 1816 | s,Q | A | $\nu$(B−$H_t$) $\nu_{17}$ ($b_1$), $\nu_2$ ($a_1$) |
| | | | | 2471 | s,P | A | 1804 | s,P | A | |
| | | 2030 | s | 2042 | w,sh | | | | | $\nu$(B−$H_b$) + ring def. $\nu_{25}$ ($b_2$), $\nu_3$ ($a_1$) |
| 2020 | s | 2015 | s | 2026 | w,sh | | | | | |
| 1992 | s | 1992 | s | 1984 | vs,Q | | 1442 | vs,br | | $\nu$(Ga−$H_t$) $\nu_4$ ($a_1$) |
| | | | | 1976 | sh | | | | | |
| 1965 | m | 1955 | s | 1971 | vs | | | | | $\nu$(B−$H_b$) + ring def $\nu_{18}$ ($b_1$) |
| | | | | 1961 | vs | | | | | |
| | | | | | | | 1390 | s | | 2 × *ca.* 700 |
| | | | | | | | 1335 | sh | | *ca.* 800 + 526 |
| | | | | 1443 | sh | | | | | |
| 1430 | s | 1435 | s | 1434 | sh | | 1041 | s | | $\nu$(Ga−$H_b$) + ring def $\nu_5$ ($a_1$), $\nu_{19}$ ($b_1$) |
| 1420 | m | 1425 | m,sh | 1417 | s,br | | | | | |
| | | | | 1319 | sh | | | | | *ca.* 914 + 400 |
| 1286 | w | 1286 | w | 1285 | mw | | 964 | m | | $\nu$(Ga−$H_b$) + ring def $\nu_{26}$ ($b_2$) |
| 1116 | m | 1120 | m | 1111 | s,br | | 848 | ms | | $B(H_t)_2$ scissoring and twisting $\nu_6$ ($a_1$), $\nu_{20}$ ($b_1$), $\nu_{27}$ ($b_2$) |
| 1102 | s | 1102 | s | | | | 841 | ms | | |
| | | 982 | w | 982 | w | | | | | impurity? |
| 770 | w | | | | | | | | | impurity? |
| | | | | 741 | mw,R | C | 536 | mw,R | C | |
| 728 | s | 735 | s | 730 | mw,Q | C | 526 | mw,Q | C | out-of-plane $B(H_t)_2$ wagging $\nu_{28}$ ($b_2$) |
| | | 724 | w | 718 | mw,P | C | 515 | mw,P | C | |
| 627 | w | 630 | w | 636 | mw,R | A | | | | |
| 609 | w | 610 | w | 628 | mw,Q | A | 472 | sh, br | | in-plane Ga−$H_t$ def. $\nu_{22}$ ($b_1$) |
| 513 | *b* | 510 | *b* | | | | | | | $[HGa(BH_4)_2]_n$ aggregate |
| | | 501 | *b* | | | | | | | $[HGa(BH_4)_2]_n$ aggregate |
| 462 | m,sh | 470 | m,sh | 473 | sh | | | | | |
| 459 | s | 465 | s | 465 | s | A | 420 | s, br | | $\nu$(Ga−B) ring def. + $\nu$(Ga−$H_b$) $\nu_{23}$($b_1$), $\nu_8$ ($a_1$) |
| 452 | w | 450 | w | 460 | sh | | | | | |

[a] Key: s, strong; m, medium; w, weak; v, very; sh, shoulder; br, broad. P, Q and R refer to branches of partially resolved rotational structure; A, B, and C, to band-types (see text). [b] Intensity varies according to conditions; increases when the matrix is annealed.

amounts of incompletely deuteriated isotopomers like $GaB_2D_8H$. While sharpening the absorptions and greatly facilitating the identification of some near-degenerate transitions, matrix isolation tended also to introduce its own complications. Thus, several of the bands were split, presumably because the $HGa(BH_4)_2$ molecules occupied different matrix sites, and although the spectrum underwent no marked changes when the matrix was annealed at temperatures up to 33 K, there was also the risk that some of the weaker features arose not from the monomer but from aggregates $[HGa(BH_4)_2]_n$. There are limitations, too, imposed partly by the low pressure of the vapor (<10 mmHg) and partly by the restricted wavenumber range of the measurements (typically 200−4000 cm$^{-1}$).

The clear doublet pattern of the absorptions near 2500 (1900) cm$^{-1}$ in the spectrum of the vapor associated with the $\nu$(B−$H_t$) fundamentals ($H_t$ = terminal H atom) is characteristic of bidentate $BH_4$ groups.[2,3,24,25] The matrix spectrum shows four distinct bands in this region, tending to confirm that all four of the $\nu$(B−$H_t$) modes are active in IR absorption, a finding consistent with the assumption that the $B(H_t)_2$ groups are coplanar with, and not perpendicular to, the $GaB_2$ framework. The antisymmetric vibrations, $\nu_1$ ($a_1$) and $\nu_{16}$ ($b_1$), are centered near 2550 (1930) cm$^{-1}$, and the symmetric vibrations, $\nu_2$ ($a_1$) and $\nu_{17}$ ($b_1$), near 2480 (1820) cm$^{-1}$, in compliance with the corresponding modes of the molecules $H_2GaBH_4$[11] and $Me_2GaBH_4$.[3] The fundamental $\nu$(Ga−$H_t$) ($a_1$) and the three IR-active $\nu$(B−$H_b$) modes ($a_1$ + $b_1$ + $b_2$) must together be responsible for the broad, intense absorption centered near 1980 (1440) cm$^{-1}$ in the spectrum of the vapor. It is difficult to know precisely how to assign the modes within this congested region of the spectrum, but the proposals contained in Tables 4 and 5 are consistent with the partially resolved rotational branches making up the complex envelope of the absorption, with the energies of related modes in the molecules $H_2GaBH_4$[11] and $Me_2GaBH_4$,[3] and with the results of the *ab initio* and DFT calculations. For each of the $\nu$(B−$H_b$) modes there is an analogous mode approximating to $\nu$(Ga−$H_b$) which is of the same symmetry. Calculations and the precedents of related molecules[2,3,11] point to the absorptions at 1434 (1041), 1417 (1041), and 1285 (964) cm$^{-1}$ as the most likely candidates for the $\nu$(Ga−$H_b$) modes $\nu_5$ ($a_1$), $\nu_{19}$ ($b_1$) and $\nu_{26}$ ($b_2$), respectively.

The $B(H_t)_2$ scissoring modes $\nu_6$ ($a_1$) and $\nu_{20}$ ($b_1$) are most plausibly allocated to the absorption centered near 1111 (845) cm$^{-1}$, in keeping with the energies of the corresponding modes in $Al(BH_4)_3$,[25] $Me_2GaBH_4$,[3] and $H_2GaBH_4$.[11] At almost the same frequency as these modes, according to the *ab initio* and DFT calculations, is the $B(H_t)_2$ twisting mode $\nu_{27}$ ($b_2$). The calculations imply similar energies and low intensities in IR absorption for the $B(H_t)_2$ in-plane rocking modes $\nu_7$ ($a_1$) and $\nu_{21}$ ($b_1$) both of which we associate with a weak feature at *ca.* 914 (700) cm$^{-1}$ displayed by the spectra of the solids. What we take to be a hybrid motion involving out-of-plane wagging of the $B(H_t)_2$ and Ga−$H_t$ units, $\nu_{28}$ ($b_2$), is most plausibly identified with a partially resolved type-C band at 730 (526) cm$^{-1}$. Evidence of a type-A contour supports the assignment of a medium-weak band at 628 cm$^{-1}$ to the corresponding in-

**Table 3.** Vibrational Spectra of Partially Annealed Solid Films of Hydridogallium Bis(tetrahydroborate) and [$^2H_9$]Hydridogallium Bis(tetrahydroborate) at Low Temperatures

| $HGa(BH_4)_2$ | | | | $DGa(BD_4)_2$ | | | | |
|---|---|---|---|---|---|---|---|---|
| IR spectrum, 77 K | | Raman spectrum, 20 K | | IR spectrum, 77 K[b] | | Raman spectrum, 20 K[b] | | |
| $\tilde{\nu}$/cm$^{-1}$ | intens[a] | $\tilde{\nu}$/cm$^{-1}$ | intens[a] | $\tilde{\nu}$/cm$^{-1}$ | intens[a] | $\tilde{\nu}$/cm$^{-1}$ | intens[a] | assignment |
| | | 2545 | m | | | | | |
| | | 2534 | vs | 1928 | s | 1930 | s | antisym. $\nu$(B−$H_t$) |
| 2526 | s | 2527 | vs | 1911 | vs | 1910 | vs | |
| | | | | 1861 | w | 1861 | w | *ca.* 1030 + 830 |
| | | | | 1838 | w | 1839 | mw | |
| 2455 | s | 2459 | vs | | | 1804 | sh | sym. $\nu$(B−$H_t$) |
| | | 2450 | vs | 1797 | vs | 1798 | vs | |
| 2378 | w | 2378 | w | | | | | *ca.* 1270 + 1110 |
| | | 2187 | mw | | | | | 2 × *ca.* 1090 |
| | | | | 1531 | m | 1532 | mw | *ca.* 830 + 700 |
| 2069 | sh | 2057 | vs | | | 1490 | s | |
| 2031 | s | 2036 | vs | 1467 | vs | 1469 | vs | |
| 2020 | s | | | 1450 | vs | | | |
| 2016 | s | | | | | 1428 | s | $\nu$(Ga−$H_t$), $\nu$(B−$H_b$) + ring def |
| 2008 | s | 2009 | s | 1405 | w | 1408 | m | |
| 2002 | s | | | 1396 | mw | 1398 | m | |
| 1991 | s | 1990 | vs | 1381 | w | 1385 | m | |
| | | 1960 | sh | | | | | |
| | | 1468 | sh | 1062 | w | 1067 | m | |
| 1450 | m | 1447 | m | 1028 | s | 1029 | m | $\nu$(Ga−$H_b$) + ring def |
| 1397 | s | 1391 | m | 1015 | sh | 1015 | m | |
| 1312 | m | 1326 | w | 987 | w | 988 | w | |
| | | 1282 | w | 963 | w | | | $\nu$(Ga−$H_b$) + ring def. |
| 1265 | m | | | 949 | m | 949 | w | |
| | | | | | | 936 | w | |
| 1212 | w,br | | | | | | | 2 × *ca.* 600 |
| | | 1140 | m | | | | | |
| | | 1126 | m | 837 | m | 840 | m | |
| 1110 | s | 1108 | mw | 829 | sh | 807 | m | $B(H_t)_2$ scissoring and twisting |
| 1089 | s | 1090 | mw | 800 | w | 802 | m | |
| | | | | | | 782 | w | |
| | | 926 | m | | | 710 | m | in-plane $B(H_t)_2$ rocking |
| 914 | w | 914 | m | 705 | vw | 700 | m | |
| | | | | 650 | w | | | *ca.* 440 + 210 |
| | | 709 | mw | 609 | w | 614 | m | |
| 699 | m | 699 | mw | 584 | w | 587 | w | |
| 682 | m | 685 | sh | | | | | Ga−$H_t$ def., out-of-plane $B(H_t)_2$ wagging |
| | | 640 | sh | | | 529 | mw | |
| 610 | m | 620 | vs | 515 | w | 517 | m | |
| | | 598 | w | 486 | m | 492 | m | |
| 561 | w | | | | | | | Ga−$H_t$ def, out-of-plane $B(H_t)_2$ wagging |
| 518 | m | 519 | s | | | 466 | s | |
| 461 | sh | 465 | vs | 446 | m | 443 | vs | |
| 440 | s | 443 | m | 414 | m | 410 | m | $\nu$(Ga−B) ring def + $\nu$(Ga−$H_b$), Ga−$D_t$ def, out-of-plane $B(D_t)_2$ wagging |
| | | | | 404 | s | | | |
| | | | | *ca.* 365 | mw,br | 382 | w | |
| | | | | | | 373 | m | |
| 400 | m | 405 | s | | | 328 | mw | Ga[($\mu$-H)$_2$$BH_2$]$_2$ bending |
| | | 396 | s | 312 | m | 312 | s | |
| 273 | w | 271 | w | *ca.* 210 | m,br | 210 | mw | Ga[($\mu$-H)$_2$$BH_2$]$_2$ twisting |
| | | 240 | w,sh | | | | | *ca.* 154 + 85 |
| | *c* | 179 | m | | *c* | 177 | m | libration |
| | *c* | 154 | s | | *c* | 145 | s | |
| | *c* | 132 | s | | *c* | 131 | m | Ga[($\mu$-H)$_2$$BH_2$]$_2$ twisting + libration modes |
| | *c* | 110 | s | | *c* | 110 | sh | |
| | *c* | | | | *c* | 102 | s, br | |
| | | | | | *c* | 85 | sh | |
| | | | | | *c* | 72 | m | |
| | *c* | *ca.* 85 | sh | | *c* | 68 | m | Ga[($\mu$-H)$_2$$BH_2$]$_2$ bending + libration modes |
| | | | | | *c* | 53 | s | |

[a] Key: s, strong; m, medium; w, weak; v, very; sh, shoulder; br, broad. [b] Some of the weaker features may be due to isotopomers of the type $GaB_2H_8D$. [c] Region not studied.

plane mode, $\nu_{22}$ ($b_1$). Out-of-plane deformation of the Ga−$H_t$ and $B(H_t)_2$ units forms the basis of a lower energy $b_2$ mode, $\nu_{29}$; on the evidence of the spectra of matrices and of solid films, this is probably located near 510 (370) cm$^{-1}$.

The region 500−380 (440−300) cm$^{-1}$ includes a relatively intense band at 465 cm$^{-1}$ which experiences only a modest shift on deuteriation (to 420 cm$^{-1}$), credentials suggesting that it approximates to the Ga···B stretching modes $\nu_8$ ($a_1$) and $\nu_{23}$ ($b_1$), although the vibrational properties of $H_2Ga(\mu\text{-}H)_2BH_2$[11,19] and the present *ab initio* and DFT calculations for $HGa(BH_4)_2$ imply a complex motion incorporating deformations of the Ga($\mu$-H)$_2$B rings. The five remaining low-energy fundamentals

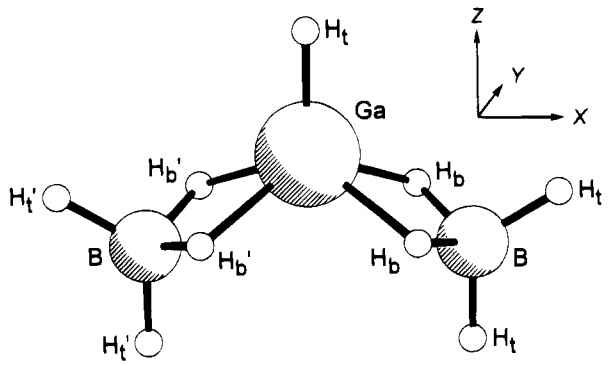


**Figure 2.** View of the $HGa(BH_4)_2$ molecule in the optimum refinement of the electron-diffraction data under $C_{2v}$ symmetry.

have been assigned mainly on the basis of the spectra characterizing solid films of the compound, with due guidance from the theoretical calculations. Bending of the $Ga[(\mu\text{-}H)_2BH_2]_2$ skeleton gives rise to two $a_1$ modes which are probably located near 400 (312) and 85 (68) $cm^{-1}$, mainly on the evidence of the Raman spectra of solid films. Twisting motions of the same skeleton form the basis of $\nu_{30}$ ($b_2$) and $\nu_{24}$ ($b_1$), and our proposed assignments of $\nu_{30}$ = *ca.* 273 (210) and $\nu_{24}$ = *ca.* 154 (110) $cm^{-1}$, also based on the spectra of solid films, are in line with the theoretical predictions. Most of the features in the spectra still unaccounted for can be interpreted satisfactorily as $a_2$ fundamentals (in the Raman spectra of the solids), as overtones or combinations of fundamentals, or as librations of the molecules within the solid lattice. As indicated by the results included in Table 5, the proposed assignments are consistent with the operation of the product rule.

**(b) Harmonic Force Field.** The observed wavenumbers of vibrational fundamentals involving Ga−H (Ga−D) and B−H (B−D) motions have been "harmonized" by using the following empirical anharmonicity constants $x_i$: $x_i$ = 0.035 for B−$H_t$ and Ga−$H_t$ stretching modes; $x_i$ = 0.030 for B−$H_b$ and Ga−$H_b$ stretching modes; and $x_i$ = 0.020 for GaH and $BH_4$ angle deformations. For the perdeuteriated molecule $DGa(BD_4)_2$, Dennison's rule[30] was assumed, *viz.* $x_i' = x_i\nu_i'/\nu_i$, in order to estimate the corresponding anharmonicity constants $x_i'$. This approach finds justification in similar treatments applied to other hydride molecules, *viz.* $B_2H_6$,[31a] $Si_2H_6$,[31b] and $H_2Ga(\mu\text{-}Cl)_2GaH_2$.[31c] Supplementary Table S1 gives a complete listing of the observed and harmonized vibrational frequencies for $HGa(BH_4)_2$ and $DGa(BD_4)_2$, together with the harmonic frequencies computed for the $C_{2v}$ structure optimized at the MP2(fc)/SV(d) and Becke3LYP/TZ(d, p) levels.

The frequencies derived from both theoretical methods are higher than those determined experimentally. For $HGa(BH_4)_2$, the root-mean-square difference between the calculated frequency and the "harmonized" experimental frequency is 39.9 $cm^{-1}$ for the *ab initio* values and 25.1 $cm^{-1}$ for the DFT values. In both cases, the overall level of agreement is pleasingly close. The improvement on going from *ab initio* to DFT is in keeping with our experience of using the density functional theory.[22,32] The discrepancies are mostly well within the range set by the approximations inherent in the theoretical methods, although there are undoubtedly some places where the experimentally derived values are far from well-defined or subject to appreciable perturbation under the action of Fermi resonance or intermolecular interactions. Hence we conclude (*i*) that the assignments we propose here are unlikely to be far wide of the mark, and (*ii*) that the vibrational spectra give no indication of asymmetric coordination of the $BH_4$ ligands or of a molecular symmetry lower than $C_{2v}$. However, a small distortion would not necessarily lead to observable changes in the spectra, and we are bound to say that the spectra are consistent with, but do not prove, $C_{2v}$ symmetry.

There is no molecule analogous to $HGa(BH_4)_2$ known to us for which normal coordinate analysis calculations have been performed, and the $C_{2v}$ structure does not lend itself to any standardized set of internal valence coordinates or symmetry coordinates. We have used the set of symmetry coordinates specified in supplementary Table S2. The molecular geometry is that deduced from the theoretical calculations (see Table 6). In view of the uncertainties affecting many of the experimentally derived vibrational frequencies, we have not attempted a detailed refinement of the theoretically based force fields, but have drawn on them to estimate vibrational amplitudes for the $HGa(BH_4)_2$ molecule. This supplementary information may be expected to aid our subsequent analysis of the remeasured electron-diffraction pattern of the gaseous molecule, and so help to determine the most realistic structure for that molecule.

**(ii) Structure of Gaseous $HGa(BH_4)_2$.** Earlier studies of this[5] and other volatile gallium hydrides[9b,10,27,33-35] or tetrahydroborate derivatives[36,37] have prepared us for the technical problems of sampling such a highly reactive and thermally fragile molecule. By changing the inlet system to one which could be more adequately preconditioned and by minimizing the fogging effects produced by the reaction of the strongly reducing vapor with the photographic plates, we have achieved a significant improvement on the results reported previously.[5]

The vibrational properties of gaseous hydridogallium bis(tetrahydroborate) are consistent with the $C_{2v}$ structure shown in Figure 2. Accordingly this model has been used to calculate electron-scattering intensities for the $HGa(BH_4)_2$ molecule. Earlier studies had tended to favor a less symmetrical ($C_2$) model characterized by *non-equivalent* Ga−$H_b$ and B−$H_b$ distances within each of the $Ga(\mu\text{-}H)_2BH_2$ moieties, and with the $BH_4$ groups twisted from their positions in the $C_{2v}$ model.[5] Refinements were therefore also carried out using such a model, in which the $BH_4$ twist parameter was defined as the torsion angle of the entire $BH_4$ group about the Ga···B axis. The total bond order for each GaHB bridge was maintained at an approximately constant value by constraining the difference between the two bridging Ga-H distances for one $BH_4$ group to be −0.7 times the corresponding difference for the bridging B-H distances. In a third series of calculations, puckering of the $Ga(\mu\text{-}H)_2B$ ring was investigated by allowing variation of a parameter $\phi$, being the angle subtended by the planes of the $Ga(H_b)_2$ and $B(H_b)_2$

(30) Dennison, D. M. *Rev. Mod. Phys.* **1940**, *12*, 175. Hansen, G. E.; Dennison, D. M. *J. Chem. Phys.* **1952**, *20*, 313.
(31) (a) Duncan, J. L.; Harper, J.; Hamilton, E.; Nivellini, G. D. *J. Mol. Spectrosc.* **1983**, *102*, 416. (b) McKean, D. C. *Spectrochim. Acta, Part A* **1992**, *48*, 1335. (c) Pulham, C. R.; Downs, A. J.; Goode, M. J.; Greene, T. M.; Mills, I. M. *Spectrochim. Acta, Part A*, in press.
(32) (a) Johnson, B. G.; Gill, P. M. W.; Pople, J. A. *J. Chem. Phys.* **1993**, *98*, 5612. (b) Jiao, H.; Schleyer, P. v. R. Unpublished results. (c) Hofmann, M.; Schleyer, P. v. R. unpublished results.
(33) Pulham, C. R.; Downs, A. J.; Rankin, D. W. H.; Robertson, H. E. *J. Chem. Soc., Dalton Trans.* **1992**, 1509.
(34) Goode, M. J.; Downs, A. J.; Pulham, C. R.; Rankin, D. W. H.; Robertson, H. E. *J. Chem. Soc., Chem. Commun.* **1988**, 768.
(35) (a) Baxter, P. L.; Downs, A. J.; Rankin, D. W. H. *J. Chem. Soc., Dalton Trans.* **1984**, 1755. (b) Baxter, P. L.; Downs, A. J.; Rankin, D. W. H.; Robertson, H. E. *J. Chem. Soc., Dalton Trans.* **1985**, 807.
(36) Barlow, M. T.; Downs, A. J.; Thomas, P. D. P.; Rankin, D. W. H. *J. Chem. Soc., Dalton Trans.* **1979**, 1793.
(37) Dain, C. J.; Downs, A. J.; Goode, M. J.; Evans, D. G.; Nicholls, K. T.; Rankin, D. W. H.; Robertson, H. E. *J. Chem. Soc., Dalton Trans.* **1991**, 967.

**Table 4.** Fundamental Modes of the $HGa(BH_4)_2$ Molecule in $C_{2v}$ Symmetry

| approx description of mode[a] | expected wavenumber range[b]/cm$^{-1}$ | $Ga(\mu\text{-}H)_2BH_2$ moiety with $C_{2v}$ symmetry irred rep[c] | $HGa(BH_4)_2$ molecule with $C_{2v}$ symmetry: irred rep[c] | no. of IR-active modes | no. of IR bands observed |
|---|---|---|---|---|---|
| antisym $\nu(B-H_t)$ | 2400−2600 | $b_1$ | $a_1 + b_1$ | 2 | 2[d] |
| sym $\nu(B-H_t)$ | 2400−2600 | $a_1$ | $a_1 + b_1$ | 2 | 2[d] |
| $\nu(B-H_b)$ + ring def and $\nu(Ga-H_t)$ | 1900−2100 | $a_1 + b_2$ | $2a_1 + a_2 + b_1 + b_2$ | 4 | ⩾3[d] |
| $\nu(Ga-H_b)$ + ring def | 1200−1500 | $a_1 + b_2$ | $a_1 + a_2 + b_1 + b_2$ | 3 | 3[d] |
| $B(H_t)_2$ scissoring and twisting | 1000−1200 | $a_1 + a_2$ | $a_1 + a_2 + b_1 + b_2$ | 3 | 2 |
| in-plane $B(H_t)_2$ rocking | 900−1000 | $b_1$ | $a_1 + b_1$ | 2 | 1[e] |
| out-of-plane $B(H_t)_2$ wagging | 700−800 | $b_2$ | $a_2 + b_2$ | 1 | 1 |
| in-plane $Ga-H_t$ def | 600−800 | − | $b_1$ | 1 | 1 |
| out-of-plane $Ga-H_t$ def | 500−700 | − | $b_2$ | 1 | 1[d] |
| $\nu(Ga-B)$ ring def + $\nu(Ga-H_b)$ | 350−500 | $a_1$ | $a_1 + b_1$ | 2 | 2[d] |
| $Ga(\mu\text{-}H)_2B$ bridge twist | <500 | $a_2$ | $a_2 + b_2$ | 1 | 1[e] |
| $Ga(\mu\text{-}H)_2BH_2$ bending | <500 | $b_1$ | $2a_1 + b_1$ | 3 | 1[e,f] |

[a] Descriptions of modes are based on those suggested for the analogous molecules $Me_2GaBH_4$,[3] $H_2GaBH_4$,[11,29] $Ga_2H_6$,[9,11] $Al(BH_4)_3$,[25] and $[H_2GaCl]_2$.[31c] Key: t = terminal; b = bridging. [b] See, for example, refs 2, 3, 9, 11, 24, and 25. [c] Irreducible representation. [d] Relates to the spectrum of the matrix-isolated molecule. [e] Relates to the spectrum of the solid. [f] Features fall largely outside the range of the current measurements.

**Table 5.** Measured Wavenumbers (in cm$^{-1}$), Assignments, and Product Rule Calculations for the Vibrational Fundamentals of the Molecules $HGa(BH_4)_2$ and $DGa(BD_4)_2$ in $C_{2v}$ Symmetry[a]

| irred. rep. | number of mode | description[b] | $HGa(BH_4)_2$ $\tilde{\nu}_H$ | $DGa(BD_4)_2$ $\tilde{\nu}_D$ | $\tilde{\nu}_H/\tilde{\nu}_D$ | $\pi(\tilde{\nu}_H/\tilde{\nu}_D)_i$[c] calcd | obsd |
|---|---|---|---|---|---|---|---|
| $a_1$ | 1 | antisym $\nu(B-H_t)$ | 2558 | 1934 | 1.3226 | 15.2665 | 14.1982 |
| | 2 | sym $\nu(B-H_t)$ | 2478 | 1816 | 1.3645 | | |
| | 3 | $\nu(B-H_b)$ + ring def | ca. 2009 | ca. 1460 | 1.3760 | | |
| | 4 | $\nu(Ga-H_t)$ | 1984 | 1442 | 1.3759 | | |
| | 5 | $\nu(Ga-H_b)$ + ring def | 1434 | 1041 | 1.3775 | | |
| | 6 | $BH_2$ scissor | ca. 1120 | 848 | 1.3208 | | |
| | 7 | in-plane $B(H_t)_2$ rock | ca. 914 | ca. 710 | 1.2873 | | |
| | 8 | $\nu(Ga\cdots B)$ ring def + $\nu(Ga-H_b)$ | 465 | 420 | 1.1071 | | |
| | 9 | $Ga[(\mu\text{-}H)_2BH_2]_2$ bending | ca. 400 | ca. 312 | 1.2821 | | |
| | 10 | $Ga[(\mu\text{-}H)_2BH_2]_2$ bending | ca. 85 | ca. 68 | 1.2500 | | |
| $a_2$ | 11 | $\nu(B\text{-}H_b)$ + ring def | ca. 1960 | ca. 1428 | 1.3725 | 4.7215 | 4.8763 |
| | 12 | $\nu(Ga-H_b)$ + ring def | ca. 1326 | ca. 963 | 1.3769 | | |
| | 13 | $B(H_t)_2$ twist | ca. 1108 | ca. 782 | 1.4169 | | |
| | 14 | out-of-plane $B(H_t)_2$ wag | ca. 640 | ca. 492 | 1.3008 | | |
| | 15 | $Ga[(\mu\text{-}H)_2BH_2]_2$ bridge twisting | ca. 154 | ca. 110 | 1.4000 | | |
| $b_1$ | 16 | antisym $\nu(B-H_t)$ | 2558 | 1934 | 1.3226 | 13.2826 | 11.8948 |
| | 17 | sym $\nu(B-H_t)$ | 2478 | 1816 | 1.3645 | | |
| | 18 | $\nu(B-H_b)$ + ring def | 1971 | 1442 | 1.3669 | | |
| | 19 | $\nu(Ga-H_b)$ + ring def | 1417 | 1041 | 1.3612 | | |
| | 20 | $BH_2$ scissor | 1111 | 844.5 | 1.3156 | | |
| | 21 | in-plane $B(H_t)_2$ rock | ca. 914 | ca. 700 | 1.3057 | | |
| | 22 | in-plane $GaH_t$ def | 628 | ca. 472 | 1.3305 | | |
| | 23 | $\nu(Ga\cdots B)$ ring def + $\nu(Ga-H_b)$ | 465 | 420 | 1.1071 | | |
| | 24 | $Ga[(\mu\text{-}H)_2BH_2]_2$ twisting | ca. 154 | ca. 110 | 1.4000 | | |
| $b_2$ | 25 | $\nu(B\text{-}H_b)$ + ring def | 2026 | 1442 | 1.4050 | 6.7950 | 6.4520 |
| | 26 | $\nu(Ga\text{-}H_b)$ + ring def | 1285 | 964 | 1.3330 | | |
| | 27 | $B(H_t)_2$ twist | ca. 1111 | 802 | 1.3853 | | |
| | 28 | out-of-plane $B(H_t)_2$ wag | 730 | 526 | 1.3878 | | |
| | 29 | out-of-plane $GaH_t$ def + $B(H_t)_2$ wag | ca. 510 | ca. 370 | 1.3784 | | |
| | 30 | $Ga[(\mu\text{-}H)_2BH_2]_2$ twisting | ca. 273 | ca. 210 | 1.3000 | | |

[a] The wavenumbers are taken from the IR spectra of the vapor, wherever possible, or otherwise from the IR and/or Raman spectra of the partially annealed solid (see text). [b] Key: $H_t$, terminal H atom; $H_b$, bridging H atom. [c] The use of observed (anharmonic) vibration frequency data is expected to give an observed product several percent *smaller* than the calculated one (see ref 14, for example). However, the discrepancy is liable to be enlarged or even reversed by the uncertainties in some of the frequencies (particularly those of the $a_2$ class which are strictly silent in IR absorption).

units. In this third refinement we assumed that both of these planes were normal to the $HGaB_2$ skeleton, in keeping with previous studies,[5] and that the $B(H_t)_2$ units had equal $B-H_t$ bond lengths as well as being coplanar with the $HGaB_2$ skeleton. Table 6 lists the independent geometrical parameters used to specify the dimensions of the $C_{2v}$ model. The parameters formed the basis of the other two models, which also included the additional parameters described above.

The radial-distribution curve, *P(r)/r vs. r*, derived from the experiments after scaling, combination, and Fourier transformation, is depicted in Figure 3. It resembles that reported earlier,[5] albeit with rather clearer definition of the region near 180 pm associated with scattering from the directly bound Ga−H atom pairs. As before, the only well-defined parameters are the *mean* B−H distance (corresponding to the peak near 120 pm), the *mean* Ga−H distance (corresponding to the peak near 180 pm), and the Ga···B distance (identifiable with the prominent feature near 220 pm). The Ga···B distance is in accord with a molecule containing dihydrogen-bridged $Ga(\mu\text{-}H)_2BH_2$ units, as in $Me_2GaBH_4$ and $H_2GaBH_4$,[10,11] rather than mono- or trihydrogen-bridged units (*cf.* $Me_2GaB_3H_8$[38] and $H_2GaB_3H_8$[33]). Since long-range atom pairs do not contribute greatly to the experimental scattering pattern, the monomer $HGa(BH_4)_2$ must be the

(38) Dain, C. J.; Downs, A. J.; Rankin, D. W. H. *J. Chem. Soc., Dalton Trans.* **1981**, 2465.

**Table 6.** Structural Parameters for $HGa(BH_4)_2$ (Distances in pm, Angles in deg)[a]

| | | electron diffraction[b] ($r_a$) | theoretical[c] ($r_e$) |
|---|---|---|---|
| | (a) Independent | | |
| $p_1$ | $r(Ga-H_t)$ | 149(4) | 154.7 |
| $p_2$ | $r(Ga-H_b)$ | 178.5(6) | 180.6 |
| $p_3$ | $r(Ga\cdots B)$ | 218.6(2) | 220.2 |
| $p_4$ | $r(B-H)$ (average) | 122.6(4) | 123.5 |
| $p_5$ | $r(B-H_b) - r(B-H_t)$ | 8.6(f) | 8.6 |
| $p_6$ | $H_tBH_t$ | 122.6(17) | 121.9 |
| $p_7$ | BGaB | 116.6(14) | 118.5 |
| $p_8$ | Pucker, $\phi$ | 3.5(f) | 3.5 |
| | (b) Dependent | | |
| | $r(B-H_t)$ | 118.3(4) | 119.1, 119.3 |
| | $r(B-H_b)$ | 126.9(4) | 127.8 |
| | $H_bGaH_b$ | 71.0(2) | 70.9 |

[a] For definitions of parameters, see text. Figures in parentheses are the estimated standard deviations. Key: f = fixed. [b] Electron diffraction of the vapor assuming $C_{2v}$ symmetry. [c] Geometry optimized using Density Functional Theory at the Becke3LYP/TZ(d, p) level.

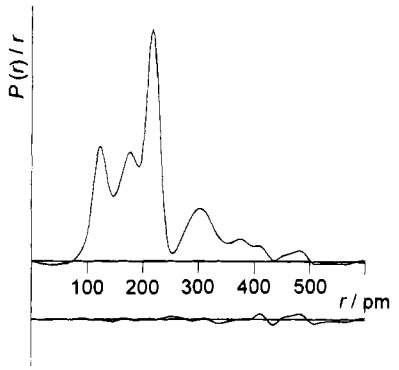


**Figure 3.** Observed and final weighted difference radial-distribution curves for $HGa(BH_4)_2$. Before Fourier inversion the data were multiplied by $s\exp[(-0.000\ 025s^2)/(Z_{Ga} - f_{Ga})(Z_B - f_B)]$.

predominant vapor species at pressures of 1−10 mmHg and near-ambient temperatures.

Full-matrix least-squares analysis[18] of molecular scattering intensities has been employed to refine the molecular structure on the basis of the three models described above. Assuming $C_{2v}$ symmetry and no puckering of the $Ga(\mu\text{-}H)_2B$ rings, six independent geometrical parameters and five amplitudes of vibration could be refined, giving $R$ factors of 0.102 ($R_G$) and 0.097 ($R_D$). The amplitudes of vibration which could not be refined were fixed at values derived from the force field calculated using the density functional theory (see below). The quality of the fit to the experimental data is markedly better than that in the previous study,[5] for which $R_G$ was 0.19 for the $C_{2v}$ model and 0.159 for the $C_2$ model. The improvement is due to the better quality of the scattering data, which resulted from our efforts to minimize contamination both of the vapor sample and of the photographic plates.

When the $C_{2v}$ constraint was relaxed, the $R$ factor was reduced both by twisting of the $BH_4$ groups and by assuming differences between bridging bond lengths within each $Ga(\mu\text{-}H)_2BH_2$ group. After a wide range of values for these parameters had been explored, both were allowed to refine. The twist angle refined to *ca.* 20°, but with a large standard deviation of 10°, while the difference between the $Ga-H_b$ bond distances converged on 6 ± 10 pm. The lowest value of $R_G$ obtained was 0.093. The symmetry was then restored to $C_{2v}$, but the constraint of planarity for the $Ga(\mu\text{-}H)_2B$ rings was removed. The puckering angle, $\phi$, refined to 10 ± 3°, with the terminal $BH_2$ groups being bent away from each other, and the BGaB angle was reduced to 110°. The $R$ factor ($R_G$) decreased by 0.008.

The $R$ factor ratios obtained with the three models imply that the twisted model with $C_2$ symmetry and the model with puckered $Ga(\mu\text{-}H)_2B$ rings both fit to the experimental data better than does the simpler $C_{2v}$ model, with 97.5% or higher significance.[39] Although neither of these distortions is reproduced by the theoretical calculations (see below), the puckering does not change the molecular symmetry, and would therefore not be detected by vibrational spectroscopy, and the distortion from $C_{2v}$ to $C_2$ symmetry, while making $a_2$ modes into IR-active a modes, would not necessarily lead to any clearly detectable changes in the spectra. The origins and significance of these apparent distortions must therefore be considered carefully.

It should be noted that the addition of extra degrees of freedom to the model can lead only to a decrease in the $R$ factor. There are two extra parameters in the $C_2$ model representing a twist of the $BH_4$ groups about their respective $Ga\cdots B$ axes and the difference between the $Ga-H_b$ bond distances, which are no longer required to be equal once the twist has been applied, coupled with a similar difference between the $B-H_b$ bond distances. Together they have led to a significant (at the 97.5% probability level) decrease in the $R$ factor. Some of this apparent distortion can undoubtedly be attributed to a shrinkage effect associated with the $a_2$ torsional mode of vibration. This mode must not be regarded as derived entirely from the torsional internal coordinate, but must incorporate components of the $a_2$ $Ga-H_b$ and $B-H_b$ stretching coordinates. Unfortunately, it is not possible to calculate reliable correction terms which would eliminate this shrinkage effect. Although perpendicular amplitude correction coefficients have been derived from the computed force field, these terms are notoriously unreliable for molecules which have large-amplitude bending modes, as in the present case. Use of such terms, which presume rectilinear rather than curvilinear coordinates, may actually introduce errors several times greater than those they purport to remove.

The results obtained using the model which allows for puckering of the $Ga(\mu\text{-}H)_2B$ rings may also be attributed to a shrinkage effect. The puckering angle refined to 10.5(30)° and the BGaB angle decreased from 119.2 to 110.4(25)°. As the overall symmetry remains $C_{2v}$, an $a_1$ mode must be responsible for the shrinkage effect. A band at 85 $cm^{-1}$ in the Raman spectrum of solid films has been assigned to a vibration of this type, which must include both ring-puckering and oscillation of the BGaB angle to account for the observed effect. Unfortunately, as before, a reliable correction could not be computed.

The results of the DFT optimization of the structure of hydridogallium bis(tetrahydroborate) in $C_{2v}$ symmetry are given in Table 6 (the Cartesian coordinates are included in the Supplementary Material). The computed values are in very good agreement with the parameters refined from the electron-diffraction data using a $C_{2v}$ model. Attempts to optimize a structure under $C_2$ symmetry did not give a new stationary point but converged to the $C_{2v}$ geometry which represents the conformation lowest in energy among the structures investigated here.[40]

A search for transition-state structures with $C_2$ symmetry led to a $C_2$ symmetric saddle point of order two, as confirmed by a frequency calculation. At the Becke3LYP/TZ(d, p) level, this structure was 50.8 kJ $mol^{-1}$ higher in energy than the $C_{2v}$ minimum. This structure consisted of only two Ga−H−B bridges, the eigenvalues of the imaginary frequencies corre-

(39) Hamilton, W. C. *Acta Crystallogr.* **1965**, *18*, 502.
(40) Similar conclusions were reached by Duke *et al.* in a theoretical investigation of $AlB_2H_9$ and $GaB_2H_9$: Duke, B. J.; Gauld, J. W.; Schaeffer, H. F., III. *Chem. Phys. Lett.*, submitted for publication.

**Table 7.** Interatomic Distances ($r_a$/pm) and Amplitudes of Vibration ($u$/pm) for $HGa(BH_4)_2$[a-c]

| | | distance | amplitude[d] |
|---|---|---|---|
| $r_1$ | Ga−$H_t$ | 149(4) | 8.8(3) |
| $r_2$ | Ga−$H_b$ | 178.5(6) | 11.9 (tied to $u_1$) |
| $r_3$ | B−$H_b$ | 126.9(4) | 7.2(5) |
| $r_4$ | B−$H_t$ | 118.3(4) | 6.2 (tied to $u_3$) |
| $r_5$ | Ga···B | 218.6(2) | 7.5(3) |
| $r_6$ | B···B | 376.4(26) | 12.7(23) |
| $r_7$ | Ga···$H_t$ | 297.3(11) | 19.4(9) |
| $r_8$ | Ga···$H_t$ | 291.0(11) | 17.9 (tied to $u_7$) |
| $r_9$ | B···$H_t$ | 320.9(16) | 14.7 (f) |
| $r_{10}$ | B···$H_b'$ | 330.5(21) | 19.4 (f) |
| $r_{11}$ | B···$H_t'$ | 479.9(22) | 14.0 (f) |
| $r_{12}$ | B···$H_t'$ | 395.6(43) | 31.0 (f) |

[a] For atom labeling scheme see Figure 2. Figures in parentheses are the estimated standard deviations. [b] H···H nonbonded distances were also included in the refinements, but are not shown here. [c] Key: f = fixed. [d] All unrefined amplitudes were fixed at the values calculated using the DFT force field. The theoretical values for the refined amplitudes are $u_1 = 9.2$, $u_3 = 9.6$, $u_5 = 6.2$, $u_6 = 13.8$, and $u_7 = 16.2$ pm.

sponding to the symmetric ($357i$ $cm^{-1}$) and asymmetric ($355i$ $cm^{-1}$) motions of the two additional hydrogen bridges in the $C_{2v}$ structure. In order to locate a true transition state for the $H_2BH_2$ rotation about the Ga-B vector, a $C_s$ structure with one $H_2BH_2$ fragment rotated by 90° was optimized. This geometry was also characterized as a second-order saddle point (38.3 kJ $mol^{-1}$ higher in energy than the $C_{2v}$ minimum). Another $C_s$ structure, with one bi- and one tridentate $BH_4$ fragment gave the $C_{2v}$ minimum structure upon normal optimization but a second-order saddle point when searching for a transition state. The latter result could not be reproduced at the MP2/SV(d) level; a transition-state search at this level, starting with the geometry optimized at the Becke3LYP/TZ(d, p) level, gave a $BH_3$·$H_2$-$Ga(\mu\text{-}H)_2BH_2$ complex, instead. Cyclic structures, of the form shown in **2**, were optimized in $C_{2v}$ and $C_s$ symmetry. These had relative energies of 40.8 and 41.7 kJ $mol^{-1}$ and three and zero imaginary frequencies, respectively. Further details of these computations are available as part of the supplementary material.

In addition, single-point energy calculations were also undertaken on the three electron-diffraction geometries discussed above. Relative to the fully relaxed theoretical geometry, the $C_{2v}$ geometries with greatly (10°) or slightly (3.5°) puckered $Ga(\mu\text{-}H)_2B$ rings gave equal relative energies of 10.9 kJ $mol^{-1}$. In marked contrast, the model geometry with $C_2$ symmetry was 43.1 kJ $mol^{-1}$ higher in energy than that of the Becke3LYP/TZ(d, p) minimum. Clearly, these DFT results favor an equilibrium structure with $C_{2v}$ symmetry.

We believe that the structure of hydridogallium bis(tetrahydoborate) does have $C_{2v}$ symmetry in the gas phase with essentially planar $Ga(\mu\text{-}H)_2B$ fragments. The apparent distortions observed by electron diffraction probably arise from large-amplitude vibrations. A final set of refinements was therefore performed with no allowance for distortions from $C_{2v}$ symmetry, but with the puckering angle, $\phi$, set at 3.5°, as calculated using DFT, and amplitudes of vibration which could not be refined fixed at values derived from the force field calculated using DFT. The parameters obtained in the final refinement are listed in Table 6, and interatomic distances and amplitudes of vibration are given in Table 7. It should be noted that the Ga−$H_t$ bond length varied over quite a wide range during the latter refinements, and it is quoted as 149(4) pm to reflect this range and give a realistic estimate of its uncertainty.

The molecular parameters calculated on the basis of the newly measured scattering patterns are mostly similar in magnitude

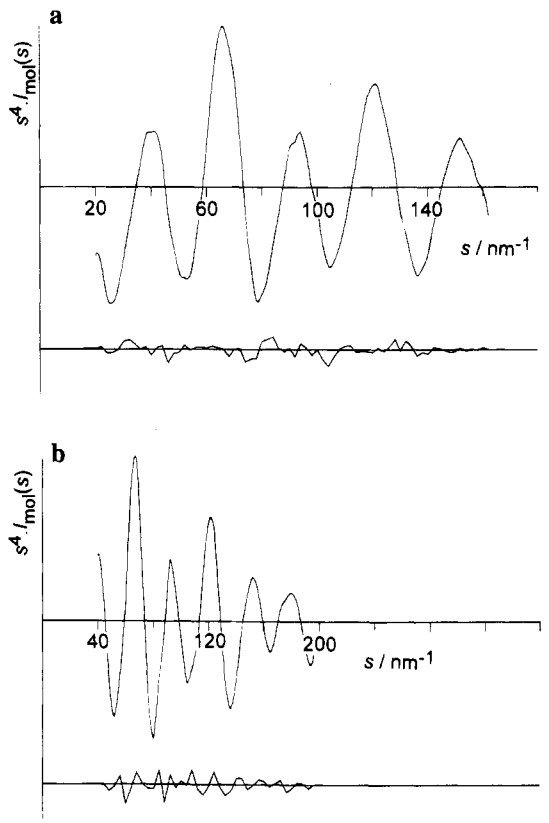


**Figure 4.** Observed and final weighted difference molecular-scattering intensity curves for $HGa(BH_4)_2$. Nozzle-to-plate distances were (a) 259.5 and (b) 201.3 mm.

to those determined previously.[5] However, the Ga−$H_b$ distance is better defined, and the Ga−$H_t$ bond length is appreciably shorter than the value deduced in the earlier study [156.5 (24) pm]. The revised estimate seems more consistent with the corresponding distances in the molecules $Ga_2H_6$ [151.9(35) pm],[9b] $H_2GaB_3H_8$ [144.2(11) pm],[33] $Me_3Ny$·$GaH_3$ [149.7(15) pm],[35a] and $[Me_2NGaH_2]_2$ [148.7(36) pm].[35b] The mean energy of the $\nu$(Ga−$H_t$) modes (in $cm^{-1}$) varies in the order $Ga_2H_6$ (1987)[9b] > $HGa(BH_4)_2$ (*ca.* 1980) > $[Me_2NGaH_2]_2$ (1885)[35b] > $Me_3N$·$GaH_3$ (1853),[41] and there is no reason therefore to expect $HGa(BH_4)_2$ to have anything but a relatively short Ga−$H_t$ bond. The B−H distances have also been refined with more success to arrive at values comparable with those in related molecules, *e.g.* $H_2GaBH_4$,[10,11] $Me_2GaBH_4$,[36] and $Al(BH_4)_3$.[42] In addition, the B−Ga−B angle has come out rather wider [116.6(14)°] than in the previous study [112.2(15)°] to give a more uniform distribution of the H and $BH_4$ ligands about the gallium atom.

The success of the analysis may be gauged from the difference between the experimental and calculated radial-distribution curves (Figure 3). Figure 4 offers a similar comparison between the experimental and simulated molecular scattering. As revealed by the uncertainties in the quoted results and the elements of the final least-squares correlation matrix reproduced in Table 8, refinement is hampered mainly by the similarity of the M−$H_b$ and M−$H_t$ distances (M = Ga or B), causing the split $\Delta r$(M−H) to be strongly correlated with the amplitudes of the M−H vectors. This correlation is the prime author of the relatively large uncertainties affecting the individual M−H

(41) Durig, J. R.; Chatterjee, K. K.; Li, Y. S.; Jalilian, M.; Zozulin, A. J.; Odom, J. D. *J. Chem. Phys.* **1980**, *73*, 21.
(42) Almenningen, A.; Gundersen, G.; Haaland, A. *Acta Chem. Scand.* **1968**, *22*, 328.

**Table 8.** Least-Squares Correlation Matrix (×100) for $HGa(BH_4)_2$[a]

| $p_2$ | $p_3$ | $p_4$ | $u_1$ | $u_5$ | $k_1$ | $k_2$ | |
|---|---|---|---|---|---|---|---|
| 77 | | 71 | | | | | $p_1$ |
| | 62 | 50 | | | | | $p_2$ |
| | | | 55 | | | | $p_3$ |
| | | | | 50 | 54 | 56 | $u_3$ |
| | | | | | 80 | 84 | $u_5$ |
| | | | | | | 75 | $k_1$ |

[a] Only elements with absolute values ≥50% are shown. $k$ is a scale factor.

bond lengths. A more precise structural specification may yet be gained from the microwave spectra of individual isotopomers. The dimensions and vibrational amplitudes determined here are subject to estimated standard deviations which allow for the effects of correlation between parameters and take account also of systematic errors in the electron wavelengths, nozzle-to-plate distances, *etc.*

**Acknowledgments.** We thank the SERC for the award of a research studentship (to C.R.P.) and research fellowships (to P.T.B., T.M.G., and H.E.R.), for financial support of the research at Oxford and of the Edinburgh Electron Diffraction Service, and for the provision of the microdensitometer facilities at the Daresbury Laboratory. We are indebted to Mr. N. Mooljee of the Edinburgh University Computing Service for technical assistance during the course of this work. We are grateful also to Drs. P. D. P. Thomas, C. J. Dain, and M. T. Barlow for their contributions to the earlier studies of hydridogallium bis(tetrahydroborate). Financial support by the Deutsche Forschungsgemeinschaft and the Volkswagenstiftung is acknowledged and also the allocation of computer time at the Höchstleistungsrechenzentrum in Jülich.

**Supplementary Material Available:** Tables of (i) observed and calculated frequencies for $HGa(BH_4)_2$ and $DGa(BH_4)_2$, (ii) the internal symmetry coordinates for $HGa(BH_4)_2$, (iii) the atomic coordinates for the final experimental and the theoretical structures of $HGa(BH_4)_2$, and (iv) theoretical relative energies and atomic coordinates of various $GaB_2H_9$ isomers are available (12 pages). Ordering information is given on any current masthead page.

IC9410250